

Electronic band states of long-range ordered aromatic thione molecules assembled on Cu(100)

Carlo Mariani

*Istituto Nazionale per la Fisica della Materia, Dipartimento di Fisica, Università di Roma “La Sapienza,”
Piazzale Aldo Moro 2, I-00185 Roma, Italy**and INFN National Center on nanoStructures and bioSystems at Surfaces (S³), Via G. Campi 213/A, I-41100 Modena, Italy*

Francesco Allegretti and Valdis Corradini

*Istituto Nazionale per la Fisica della Materia, Dipartimento di Fisica, Università di Modena e Reggio Emilia,
Via G. Campi 213/A, I-41100 Modena, Italy*

Giorgio Contini

CNR-ITM, via Bolognola 7, I-00138 Roma, Italy

Valeria Di Castro

*Istituto Nazionale per la Fisica della Materia and Dipartimento di Chimica, Università di Roma “La Sapienza,”
Piazzale Aldo Moro 2, I-00185 Roma, Italy*

Chiara Baldacchini and Maria Grazia Betti

*Istituto Nazionale per la Fisica della Materia, Dipartimento di Fisica, Università di Roma “La Sapienza,”
Piazzale Aldo Moro 2, I-00185 Roma, Italy*

(Received 17 April 2002; published 10 September 2002)

Two-dimensional long-range ordered organic molecule layers can be achieved by depositing thiols on single crystalline surfaces. The aromatic thione 2-mercaptobenzoxazole (MBO) molecule (C_7H_5NOS) presents a S-containing head which reacts with the Cu surface, and an aromatic ring originating lateral van der Waals interactions and molecular self-organization. A long-range-ordered $p(2 \times 2)$ structure of MBO on Cu(100) is obtained, by MBO sublimation in highly controlled ultrahigh-vacuum conditions. The MBO molecular orbitals and interface electronic levels have been identified, also comparing the room-temperature experiment with the low-temperature (100 K) physisorption data, by angular-resolved high-resolution UV photoelectron spectroscopy. The role of S as a chemical hook for the molecule to the Cu surface is evidenced, and comparison with similar compounds suggests that the adsorption mechanism and the related electronic structure are rather general results for π -conjugated molecules with a S-containing head. We give striking evidence of energy-band formation of MBO-Cu interaction states, bringing to light molecule-Cu extended hybrid bands, with a bandwidth of 120 meV along one main azimuthal symmetry direction of the surface Brillouin zone.

DOI: 10.1103/PhysRevB.66.115407

PACS number(s): 73.20.-r, 71.20.-b, 79.60.Fr

I. INTRODUCTION

A growing and strong interest in organic molecule deposition on surfaces has been recently stimulated by the realization of prototype devices in view of the “plastic electronics” era.^{1,2} For example, it has been shown how a monolayer of thiolates or appropriately modified benzene dithiolate molecules deposited on suitable substrates can give rise to resonant-tunneling transistors.³⁻⁶ Despite the growing interest in such systems, still open questions remain about the intimate molecule-to-substrate interface properties, the evolution of the electronic molecular levels (formation of extended band states, bandwidth), the conduction mechanisms at the molecular scale (electron-phonon interaction and polaron effects), and microscopic control of the transport properties.

Electrical conductivity in these systems is generally driven by the π -conjugated rings, allowing electron delocalization via π stacking, which plays an important role in charge transport for organic and also biological systems.⁷⁻⁹

Several organic molecules incorporate the aromatic ring in the molecular body, and can be tethered to noble-metal surfaces through external atoms (such as sulfur): organic thiols and thiones belong to this class of self-assembling molecules on surfaces.¹⁰⁻¹⁵ Adsorption of aromatic organic molecules at surfaces can take place *via* the aromatic ring interaction with the substrate, such as with benzene^{16,17} or polyacenes,¹⁸ resulting in a modification of π conjugation due to new bonding configurations, compromising their transport properties. On the contrary, thiol and thione molecule adsorption is based on a chemical strategy involving molecule-to-substrate interaction *via* specific functional groups which are not an intrinsic part of the delocalized π system.¹⁹⁻²² In fact, the S-containing head reacts with the surface, while the aromatic ring generates lateral van der Waals interactions driving the molecular self-organization and packing, opening a possible charge conduction channel.^{3,6,9}

The type of molecule-to-substrate interaction, the identification of the electronic interface states, and possible extended band formation are still open questions, despite the

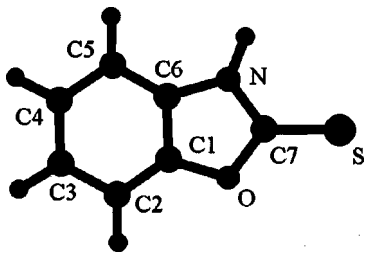


FIG. 1. Sketch structure of the 2-mercaptobenzoxazole (C_7H_5NOS , MBO) molecule in the thione form (see text).

deep interest in the study of two-dimensional ordered assembly of organic molecules with aromatic groups, and of their packing and effects on electronic interactions.

In this context, this work focuses on the experimental determination of extended electronic band formation at organic molecule ordered layers adsorbed on surfaces. We obtain the surface band structure and parallel momentum dispersion with high-energy-resolution UV photoemission, by depositing the 2-mercaptobenzoxazole (C_7H_5NOS , in the following MBO) molecule on Cu(100), in the typical conditions of surface science standard. This molecule, whose linear dimensions are roughly $7.2 \times 4.8 \text{ \AA}^2$,²³ presents an aromatic part and an etheroatomic ring, with a S atom as the chemical “arm” (Fig. 1). Thin layer MBO deposition in UHV conditions has been studied on Pt(111) by near-edge x-ray absorption fine-structure spectroscopy,^{24,25} and on Cu(100) single crystals by scanning tunneling microscopy,²³ showing the formation of ordered phases, allowing the determination of the average molecular orientation and the strong molecule-to-substrate interaction by the S atom.

We hereafter present an angular-resolved high-resolution UV photoelectron spectroscopy (AR-HRUPS) investigation of the room-temperature (RT) MBO adsorption on the Cu(100) surface in UHV. The molecule layer forms a long-range-ordered $p(2 \times 2)$ superstructure. We show how the S atom acts as a hook for the molecule tethering at the noble-metal surface, identifying the molecule-to-substrate interaction levels and interface electronic states. In particular, we give strong evidence of energy-band formation for an adsorbed oligomer organic system, bringing to light molecule-Cu hybrid extended bands, whose dispersion is clearly measured along the main symmetry directions of the surface Brillouin zone (SBZ).

II. EXPERIMENT

The experiments, carried out at the surface physics laboratory LOTUS, were performed in UHV chambers containing an angular-resolved high-resolution ultraviolet photoelectron spectroscopy apparatus, low-energy electron diffraction (LEED), and other ancillary facilities for sample preparation.

All photoelectron spectra reported here were excited with a high-intensity He discharge lamp (He $I\alpha$ and He $II\alpha$ photons, $h\nu = 21.218$ and 40.814 eV, respectively). The photoemitted electrons were analyzed in the plane of incidence, with a high angular- and energy-resolution Scienta SES-200

hemispherical analyzer, equipped with angle and energy parallel two-dimensional detection by a multichannel plate, with an angular resolution better than 0.2° . The angular detection range spans $\pm 8^\circ$ with respect to the spectrometer lens axes. Wider angular limits, to reach the SBZ boundary, were achieved by rotating the crystal surface normal with respect to the spectrometer lens axes. Angular-integrated spectra were taken with an integration angle of about $\pm 6^\circ$ with respect to the normal-emission direction. A good compromise between signal-to-noise ratio, good energy resolution, and acquisition time was obtained using 2 eV (10 eV) pass energy and 0.8-mm slits in the angular-integrated (-resolved) mode. In these conditions, the energy resolution was 16 meV (24 meV), as determined on the Fermi level (E_F) of Cu. Calibration of the binding energy (BE) scale with respect to the measured kinetic energy was carried out in the adsorbed systems, using the Cu Fermi edge at 0 eV BE.

The high-purity (99.999%) Cu(100) single crystal was repeatedly cleaned by a series of sputtering-annealing cycles in order to remove the contaminants (carbon, oxygen, and sulfur) from the sample surface. After the cleaning procedure, the Auger spectra showed contaminant signals well below the noise level. Each cleaning cycle consisted of sputtering with Ar^+ ions (800 eV, 8 μA for 30 min), followed by annealing at 690 K for a few minutes. Flash at higher temperature (about 30 s at 740 K) induced larger coherence domains of the surface, as evidenced by the sharper LEED pattern.

The MBO molecule was supplied by Aldrich Chemical Company Inc. in the form of powder, with 98.4% purity determined by gas chromatography analysis. The main impurities, crystallization solvents, were removed before the insertion in the experimental chamber, by repeated sublimation cycles. The molecule was contained in a retractable stainless-steel cylinder, UHV connected to the preparation chamber with a leak valve. The MBO molecule was sublimated by heating the cylinder at 390 K, after repeated heating-pumping cycles for further cleaning. The molecule can exist in two tautomeric forms, the thione with NH (used in this work, reported in Fig. 1) and the thiol form with SH. The thione form presents a $C=S$ double bond, while the thiol form has the endocyclic double bond $C=N$ and the hydrogen atom bonded to the sulfur atom instead of the nitrogen. Among the two tautomeric forms of this molecule, only the thione form is present in the MBO vapor while sublimating it in UHV conditions, as ascertained by previous x-ray absorption and photoemission spectroscopy.^{25,26}

All the depositions were carried out at a comparable value of the MBO pressure (in the 10^{-6} -Pa range), only varying the exposition time, to avoid effects of different adsorption rates on the growth morphology. The exposures were measured in Langmuir units ($1 L = 1.33 \times 10^{-4}$ Pa s). We observed a variation of the actual deposition rate—at constant exposure—depending on the partial MBO pressure. However, this effect does not substantially influence the growth morphology at RT, but hinders the use of the exposure as a comparative quantity. Since saturation was observed in the photoemission experiment at RT, we use the saturation coverage (Θ_{sat}) as the deposition quantity for the data taken at

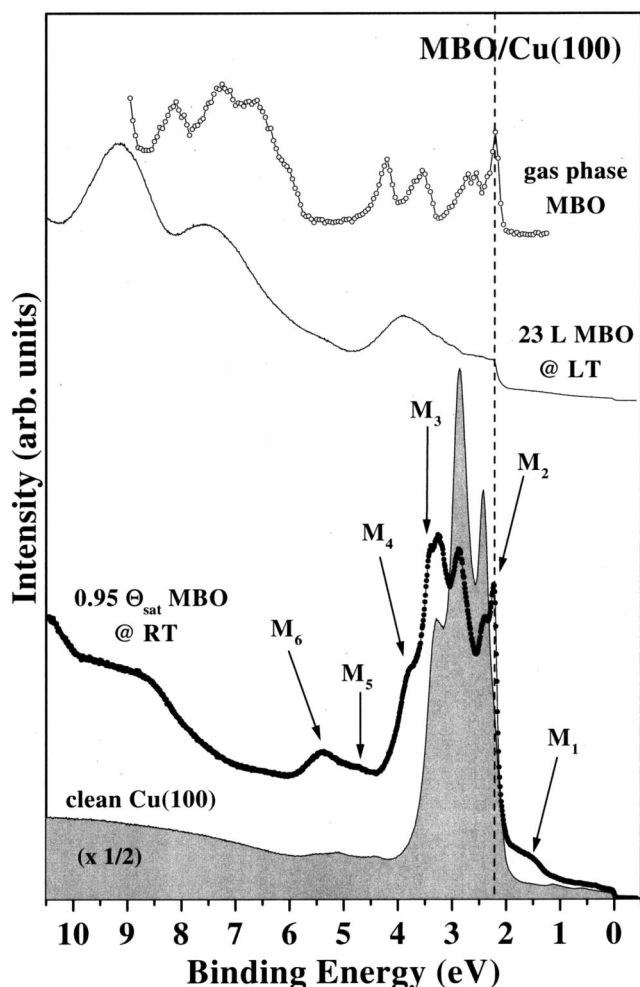


FIG. 2. High-resolution UV (He I photon energy, 20.218 eV) angular-integrated photoemission spectra of 2-mercaptobenzoxazole (MBO) deposited on Cu(100) at 298 K (RT, 0.95 of saturation coverage) and at 100 K (LT, 23 L multilayer deposition). Data from the clean Cu(100) surface and from gas-phase MBO (from Ref. 26) are shown for comparison. The major MBO-induced structures are indicated (M_1 – M_6).

room temperature. In general, the lower the deposition rate, the better order was obtained.

III. RESULTS AND DISCUSSION

A. Valence band at condensed and at chemisorbed MBO

A propaedeutic task for the understanding of the MBO interaction at the single crystal Cu(100) surface is the comparison between photoemission data at the gas phase, physisorbed phase (at 100 K), and room temperature deposited MBO, with the goal to discriminate between molecular and molecule-to-substrate interaction states. For this purpose, angular-integrated valence-band photoemission data of MBO deposited on the Cu(100) surface at room (298 K) and low (100 K) temperature have been taken, and shown in Fig. 2, along with the clean Cu data and MBO gas-phase spectra.²⁶

The latter spectrum is calibrated against the C 1s signal of the benzenelike atoms (C_3 and C_4 in Fig. 1) at 285.0 eV.

MBO sublimation on the substrate kept at low temperature (LT) gives rise to the first layer chemically interacting with the substrate and characterized by interface electronic states, followed by a multilayer condensed phase, where the molecule-Cu states disappear and more proper molecular orbitals emerge, as reported in Ref. 27. The first interacting layer formed at LT resembles the room-temperature adsorption data, which we shall discuss later.

The uptake of MBO in the condensed phase is continuous, with the formation of a multilayer film, on top of the first MBO-Cu interacting layer.²⁷ The low-temperature angular-integrated data (Fig. 2) obtained for multilayer MBO grown on Cu(100) present valence-band features with main structures at 2.20, 3.85, 7.55, and 9.15 eV BE, with wider shoulders at ~ 2.6 and ~ 3.1 eV. These peaks, characteristic of a physisorbed phase, can be analyzed in close relation with those of the gas-phase spectrum and related calculations.²⁶ In particular, the peak at 2.20 eV can be assigned to the highest occupied molecular orbital (HOMO), well identified in the gas-phase data and attributed to a π delocalized orbital, while the wide shoulder at ~ 2.6 eV can be correlated to the HOMO-1 orbital mainly localized on the S atom of the MBO molecule. The wide asymmetric BE structure centered at ~ 3.85 eV, with the shoulder at ~ 3.1 eV, can be assigned to the two molecular states associated to highly delocalized π orbitals (3.56 and 4.22 eV) in the gas phase, broadened and shifted by the adsorption in the condensed phase. The highest BE peaks at 7.55 and 9.15 eV come from the convolution of a variety of molecular orbitals with different origin, and are broadened and shifted in the condensed phase.

Once the MBO molecular orbitals in the valence band of physisorbed MBO are established, we analyze the room-temperature MBO adsorption on Cu(100). The angular-integrated valence-band data (Fig. 2) present six main MBO-derived structures (M_1 at 1.50 eV, M_2 at 2.23 eV, M_3 at 3.40 eV, M_4 at 3.80 eV, M_5 at 4.75 eV, and M_6 at 5.35 eV BE), and the Cu 3d band structure with reduced intensity. We show in Fig. 2 (bottom part) the spectrum at about 0.95 of the saturation coverage, corresponding to a good $p(2 \times 2)$ LEED diffraction pattern. Data from the very first coverage phases present an analogous distribution of these valence-band features, in particular, the main structures maintain their shape and position.

The peak at 1.50 eV BE (M_1 in Fig. 2) has an intensity increasing with the coverage, and it becomes more evident with respect to the other MBO-induced structures by using He II α photons (40.418 eV photon energy). According to atomic excitation cross-section considerations,²⁸ where the Cu d -symmetry level cross section increases from 7.2 to 9.9 Mb upon changing the photon energy from He I to He II, while the S 3p cross section decreases from 4.3 to 0.6 Mb close to its Cooper minimum, we attribute this structure to an antibonding MBO-Cu S 3p–Cu 3d, 4s hybrid state, with the major contribution of d -symmetry states. Our attribution can be confirmed by previous S/Cu(100) photoemission data,^{29,30} and by photoemission and electron-energy-loss spectroscopy studies on alkanethiols³¹ and benzenethiols^{32,33}

chemisorbed on Cu, where the adsorbate-substrate bonding proceeds *via* formation of new bonding and antibonding states between the Cu $3d_{xz,yz}$ -S $3p_{x,y}$ and Cu $4s/3d_{z^2}$ -S $3p_z$ orbitals.

The feature at 2.23 eV (M_2 in Fig. 2) is absent on the clean Cu surface, its intensity is appreciable for coverages roughly above $0.6 \Theta_{\text{sat}}$. It is clear and close to the structures observed for the gas phase and the low-temperature condensed molecular phase, thus it is not related to the molecule interaction with the substrate, rather to proper molecular states. We can reasonably attribute this peak to the HOMO molecular orbital of the MBO, mainly localized on the rings' π bonds, and basically unperturbed due to the major S interaction with the substrate.

The peak at 3.40 eV (M_3 in Fig. 2), very close to the residual Cu $3d$ band signal, is reasonably due to π -delocalized molecular orbitals observed in the gas-phase data. The clear shoulder at 3.80 eV (M_4 in Fig. 2) is absent on the clean substrate, its intensity decreases with the photon energy,²⁷ and a similar feature is present at ~ 3.85 eV in the condensed phase, deriving from the merging of two gas-phase features. However, a similar structure observed in previous photoemission data on S chemisorption on Cu(100) (Ref. 30) is assigned to a S interface state, thus its attribution remains uncertain.

The two structures at 4.75 and 5.35 eV BE (M_5 and M_6 in Fig. 2) are neither present in the clean surface, nor in the condensed and gas-phase MBO data, and appear from the lowest coverage values. Their intensity decreases with the photon energy, in comparison with the other structures, so that considerations on the atomic excitation cross section²⁸ lead us to associate them with S $3p$ derived states interacting with the Cu levels. Analogous clear structures are present in the S (Refs. 29 and 30) and thiol³¹⁻³³ chemisorption on Cu(100), and we consistently attribute them to the bonding S $3p_z$ (4.75 eV) and S $3p_{xy}$ (5.35 eV) levels hybridized with Cu states. These features, more clearly the M_6 peak, present a clear dispersion in parallel momentum, as we shall see in the following section, marking the importance of the MBO interaction with Cu upon chemisorption. The previous discussion on the electronic levels and on the observed $p(2 \times 2)$ reconstruction suggests that the sulfur atom of the MBO molecule plays a major role in the chemisorption process with Cu at room temperature, acting as a chemical hook for the regular aggregation of this molecule on the surface.

We briefly mention that the MBO chemisorption phase on Cu(100) is stable as a function of temperature by warming up the system up to 450 K, higher than the MBO sublimation temperature (~ 385 K). This spectral stability characterizes the MBO-Cu interaction as stronger than the intermolecular interaction leading to the condensed phase.

B. Surface symmetry and electronic band structure of the chemisorbed MBO/Cu(100) system

The MBO molecule forms a long-range ordered structure when it is chemisorbed on the Cu(100) surface at room temperature, with a $p(2 \times 2)$ reconstruction throughout the whole coverage range, as shown by the low-energy diffrac-

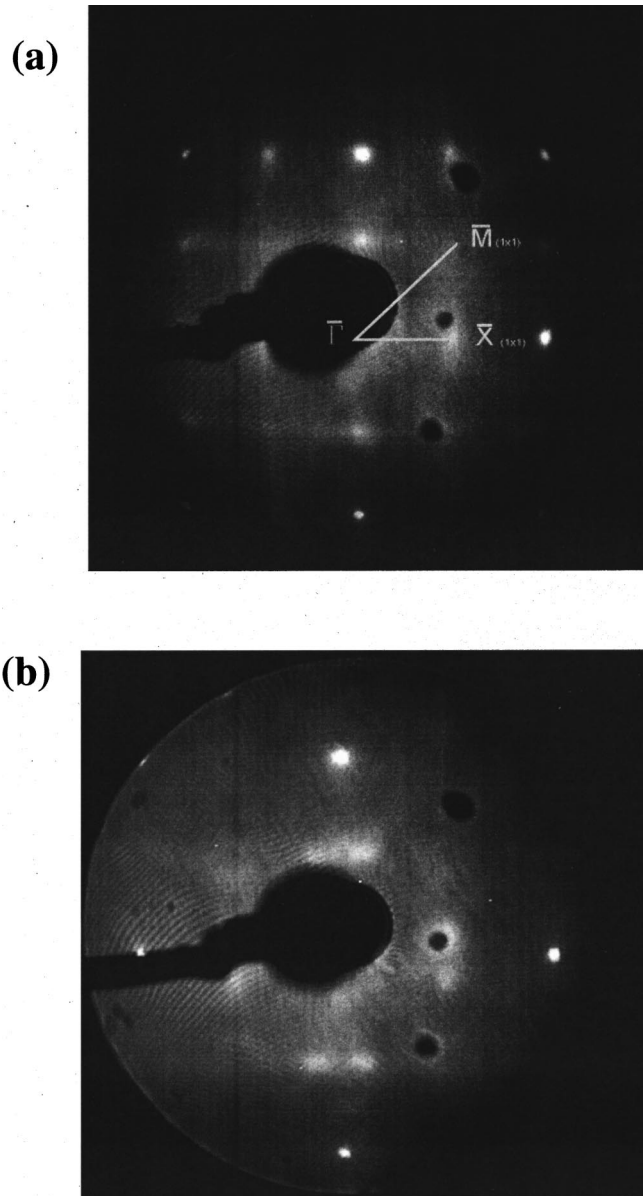


FIG. 3. Low-energy electron diffraction (LEED) pattern of the $p(2 \times 2)$ -reconstructed MBO-Cu(100) system, at two different MBO depositions at room temperature: (a) $0.71\Theta_{\text{sat}}$ (pattern image taken at 93 eV), with the sketch of the main symmetry directions and points of the (1×1) surface Brillouin zone (SBZ); (b) $0.95\Theta_{\text{sat}}$ (pattern image taken at 65 eV). Note the splitting of the double-order LEED diffraction spots for a deposition close to saturation coverage.

tion pattern image plotted in Fig. 3(a). However, the double-order diffraction spots in the LEED pattern widen in streaky segments above roughly $0.7\Theta_{\text{sat}}$, which eventually develop in a double spot along the two equivalent $[001]$ and $[010]$ symmetry directions, with an increased diffused background at saturation coverage [Fig. 3(b)]. This double-spot pattern may arise from equivalent antiphase domains. In fact, assuming that the S atoms tethering the MBO molecule to the Cu(100) surface adopt a fourfold symmetry analogous to that of S chemisorbed on the same surface,³⁴⁻³⁷ equivalent an-

tiphase domains can form on the (100) surface. The antiphase domain boundaries with a random distribution of dimensions can give rise to the streaky LEED pattern, and to a slightly different binding energy of the S core levels for atoms either in the domains, or at the interdomain boundaries.³⁸ Upon approaching saturation coverage at RT, the antiphase domains compact and order, generating a domain commensurate superlattice that can be equivalently present along the two surface directions, thus giving rise to the double-spot structure along both the [001] and [010] directions. Another possible explanation of the spot doubling in the LEED pattern may be the presence of commensurate missing rows of the adsorbed molecules in equivalent domains along the two symmetry directions. A conclusive assignment deserves specific structural investigation of the molecule adsorption geometry.

An AR-HRUPS experiment has been carried out at the $p(2 \times 2)$ ordered $0.95\Theta_{\text{sat}}$ MBO layer chemisorbed on Cu(100) at room temperature, along the two main symmetry directions of the (1×1) SBZ [$\overline{\Gamma X}$ and $\overline{\Gamma M}$, sketched in Fig. 3(a)]. A selection of these AR-HRUPS spectra is plotted in Fig. 4, while a pictorial view of the data is shown in Fig. 5 in a projected three-dimensional plot, as a function of the photoelectron collection polar angle along the two azimuthal directions. Lines superimposed on the image correspond to the main peak positions; in particular, the molecule-induced states are labeled as M_i peaks.

After a comparison of these energy-dispersion data with the measured clean Cu(100) projected band structure, we observe the disappearance of the Cu surface states, particularly the Tamm and Schockley surface peaks.^{39–43} The residual signal of the Cu projected bulk structure, namely, the residual s - p dispersing band with an almost parabolic shape, some less dispersive features due to the Cu $3d$ bands in the 2–4 eV BE range, and ds -like states at higher BE are reported with white dots in Fig. 5. The molecule-induced and MBO-Cu interaction states, well identified at the (1×1) SBZ boundary, are resonant with the Cu projected bulk bands in the vicinity of $\overline{\Gamma}$. In the low BE region, apart from the Cu sp band, we can observe the nondispersive MBO M_1 level (~ 1.5 eV BE at $\overline{\Gamma}$).

Generally, all the molecule-induced states present a tiny dispersion, indicating a rather localized nature of the electronic levels. The lowest BE level is M_1 , whose origin is based on the interaction between the S atom of the MBO molecule and the substrate atoms, with hybridization of S $3p$ -Cu $3d, 4s$ bonds, and major d -orbital contribution. M_2 is a structure due to MBO molecular orbitals, associated to π -like levels extending throughout the whole SBZ, and M_3 is an MBO derived level, partially hidden by the d bands towards the $\overline{\Gamma}$ point, probably related to the 3.56-eV gas-phase molecular orbital. These two orbitals (M_2 and M_3) are delocalized within the single molecule, while only a very tiny intermolecular interaction can be invoked for them, given their low dispersion. M_a , M_b , and M_c can be assigned to the presence of MBO, as Cu does not present any state in this energy range at the \overline{M} point of the SBZ, where these levels are more evident. The origin of these levels is

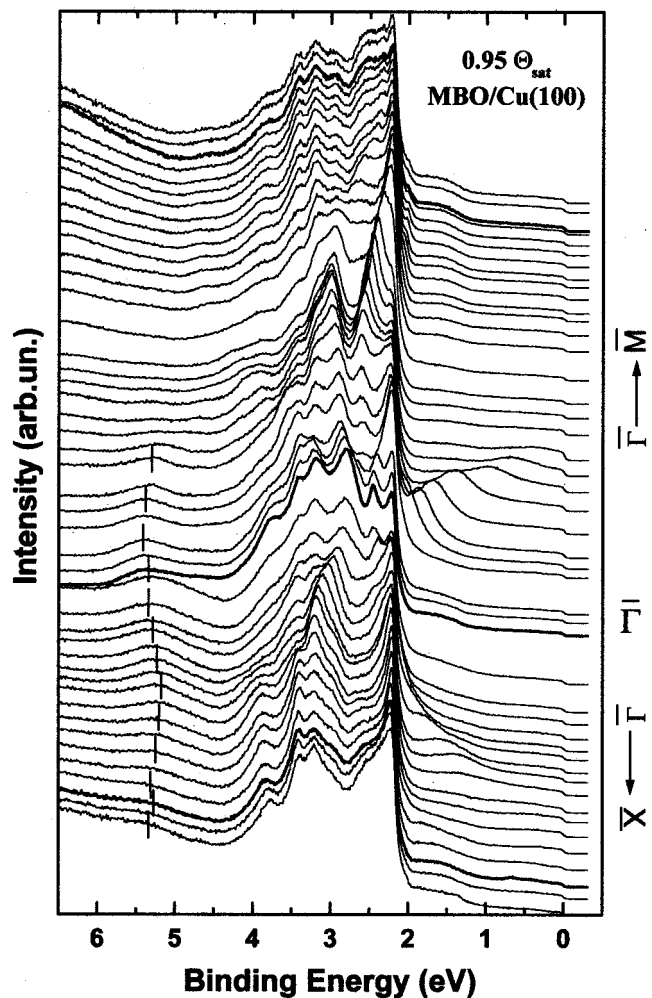


FIG. 4. Angular-resolved high-resolution UV (He I photon energy, 20.218 eV) photoemission data of $0.95\Theta_{\text{sat}}$ 2-mercaptobenzoxazole (MBO) chemisorbed on Cu(100) at room temperature (298 K), as a function of the photoelectron emission angle (from 0° to 69° polar angle along $\overline{\Gamma M}$, and from 0° to 42° polar angle along $\overline{\Gamma X}$). Selection of spectra, with the indication of the corresponding main SBZ directions (thick-line spectra approximately correspond to the \overline{M} and \overline{X} points).

not straightforward, however they can be due to an interaction orbital of the molecule with the substrate. The electronic state M_4 is clearly distinguishable at the SBZ center and along the $\overline{\Gamma M}$ direction, and due to the presence of the MBO molecule. A structure at the same energy is also present in the gas-phase MBO data, and a similar peak has been observed at the S/Cu(100) interface.³⁰ Though its origin is uncertain, due to its slight energy dispersion we tentatively attribute it to an S-Cu interface state.

The most interesting MBO-Cu electronic states are M_5 and M_6 , whose energy dispersion can be clearly observed along the $\overline{\Gamma X}$ direction. As previously discussed, we assign both to S $3p$ derived states interacting with the Cu bands. Their energy dispersion is plotted in Fig. 6, as a function of the parallel momentum k_{\parallel} along the $\overline{\Gamma X}$ symmetry direction of the (1×1) SBZ. In particular, we can clearly follow the

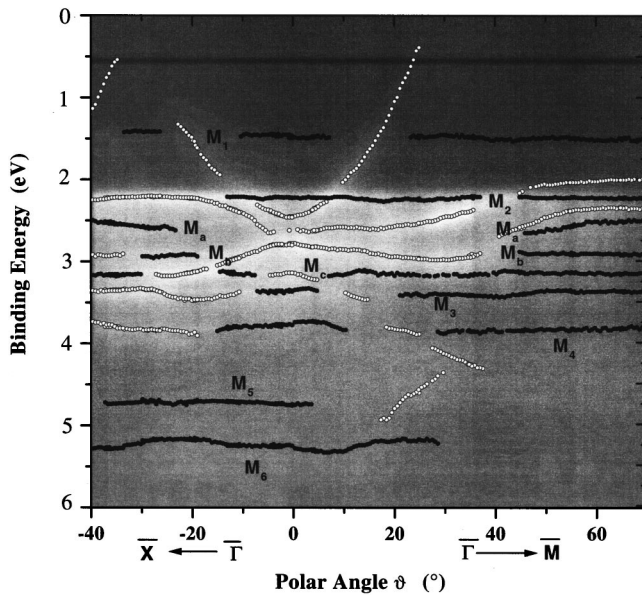


FIG. 5. Energy-band dispersion of the MBO-induced states at $0.95\Theta_{\text{sat}}$ $p(2\times 2)$ MBO/Cu(100) as a function of the polar angle [negative angles correspond to the $\overline{\Gamma X}$ direction, positive angles to the $\overline{\Gamma M}$ direction of the (1×1) SBZ]. Projected three-dimensional plot, with the intensity represented in false gray scale, and the main peak position reported as data points (white points, Cu bulk-projected bands; black dots, molecule-Cu interaction states). The highest-intensity bands in the 2.2–3.5 eV binding energy range are due to the Cu projected bulk d states.

M_6 dispersion along $\overline{\Gamma X}$, where no any other Cu derived structures are present, while the M_5 dispersion is affected by a larger error (± 50 meV). The M_6 energy band presents an evident symmetry with respect to half the (1×1) SBZ $\overline{\Gamma X}$ direction, as shown in Fig. 6, with a bandwidth of (120 ± 15) meV. The symmetry doubling in the real space is in agreement with the observed $p(2\times 2)$ reconstruction of the MBO-Cu(100) system. The energy dispersion of the molecular-induced states clearly indicate a molecule-molecule interaction via the S atoms bonded to the Cu surface, so as to determine a substrate-mediated molecular interaction. A previously reported angular-resolved photoemission study of $p(2\times 2)$ sulfur adsorbed on Cu(100) could not determine any clear dispersion below 200 meV,³⁰ nor band dispersion was evidenced by previous ARUPS studies on organic thiols chemisorbed on metal surfaces. To our knowledge, this is a striking experimental evidence that organic monolayers of oligomers, long-range ordered at a single crystalline surface, induce extended electronic band formation.

IV. CONCLUSIONS

Molecular MBO and interface MBO-Cu electronic levels have been identified at chemisorbed 2-MBO on Cu(100), deposited by controlled sublimation in ultrahigh-vacuum conditions, by angular-resolved high-resolution UV photoelectron spectroscopy, and also analyzing the low-temperature

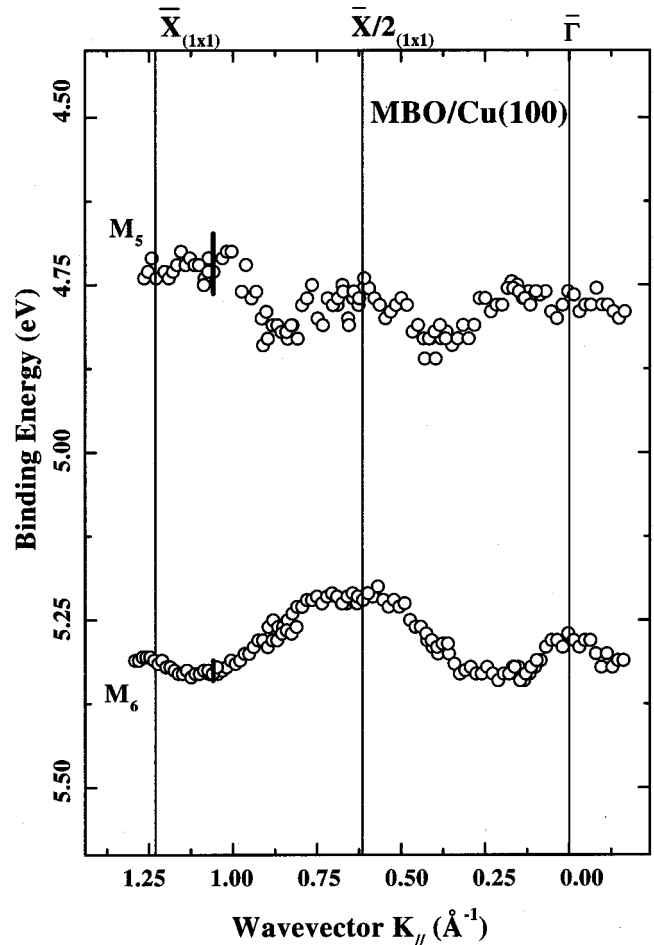


FIG. 6. Energy-band dispersion of the M_5 and M_6 electronic levels of $0.71\Theta_{\text{sat}}$ $p(2\times 2)$ MBO/Cu(100), as a function of the parallel momentum k_{\parallel} along the main symmetry direction $\overline{\Gamma X}$ of the (1×1) SBZ.

adsorption of condensed MBO. The role of S as a tethering agent in the process of MBO chemisorption has been brought to light, by studying the interaction of its orbitals with the noble-metal substrate. We identify MBO-derived electronic levels presenting a definite energy-band dispersion of 120 meV, with doubled symmetry in the reciprocal space along the surface Brillouin zone (in agreement with the observed 2×2 reconstruction), suggesting a molecule-to-molecule interaction mediated by the bond to the substrate surface atoms. The molecule contains an S atom, whose interaction with the noble-metal surface for establishing bond, order, and extended electronic state formation can be addressed as a general feature of chemisorbed thiols and thiol-like molecules. Moreover, the high-resolution ARUPS proved to be the best suited and tailored spectroscopic technique for the direct determination of molecule-induced energy-band dispersion at ordered layers of chemisorbed organic molecules.

ACKNOWLEDGMENTS

Financial grants from Ministero per l'Università e per la Ricerca Scientifica e Tecnologica (MURST) under confin2000 and ex-60% programs, and from Consiglio Nazionale delle Ricerche (CNR) are gratefully acknowledged.

- ¹Jairo Sinova, John Schliemann, and Alvaro S. Nunez, *Phys. Rev. Lett.* **87**, 226802 (2001).
- ²Franck-J. Meyer zu Heringdorf, M. C. Reuter, and R. M. Tromp, *Nature (London)* **412**, 517 (2001).
- ³M. A. Reed, C. Zhou, C. J. Muller, T. P. Burgin, and J. M. Tour, *Science* **278**, 252 (1997).
- ⁴M. Di Ventura, S. T. Pantelides, and N. D. Lang, *Appl. Phys. Lett.* **76**, 3448 (2000).
- ⁵Jan Hendrik Schön, Hong Meng, and Zhenan Bao, *Nature (London)* **413**, 713 (2001); **414**, 470(E) (2001).
- ⁶X. D. Cui, A. Primak, X. Zarate, J. Tomfohr, O. F. Sankey, A. L. Moore, T. A. Moore, D. Gust, G. Harris, and S. M. Lindsay, *Science* **294**, 571 (2001).
- ⁷M. R. Arkin, E. D. A. Stemp, R. E. Holmlin, J. K. Barton, A. Hormann, E. J. C. Olson, and P. F. Barbara, *Science* **273**, 475 (1996).
- ⁸P. Aich, S. L. Labuik, L. Tari, L. J. T. Delbaere, W. J. Roesler, K. J. Falk, R. P. Steer, and J. S. Lee, *J. Mol. Biol.* **294**, 477 (1999).
- ⁹Rosa Di Felice, Arrigo Calzolari, Elisa Molinari, and Anna Garbesi, *Phys. Rev. B* **65**, 045104 (2002).
- ¹⁰A. Ulman, *Chem. Rev.* **96**, 1533 (1996).
- ¹¹F. Schreiber, *Prog. Surf. Sci.* **65**, 151 (2000).
- ¹²G. E. Poirier and E. D. Pylant, *Science* **272**, 1145 (1996).
- ¹³R. Staub, M. Toerker, T. Fritz, T. Schmitz-Hübsch, F. Sellam, and K. Leo, *Langmuir* **14**, 6693 (1998).
- ¹⁴G. E. Poirier, *Langmuir* **15**, 1167 (1995).
- ¹⁵S. Hasegawa, T. Horigome, K. Yakushi, H. Inokuchi, K. Okudaira-Kamiya, N. Ueno, K. Seki, R. J. Willicut, R. L. McCarley, E. Morikawa, and V. Saile, *J. Electron Spectrosc. Relat. Phenom.* **113**, 101 (2001).
- ¹⁶Maynard J. Kong, Andrew V. Teplyakov, Julia G. Lyubovitsky, and Stacey F. Bent, *Surf. Sci.* **411**, 286 (1998).
- ¹⁷Brian Borovsky, Michael Krueger, and Eric Ganz, *Phys. Rev. B* **57**, R4269 (1998).
- ¹⁸S. Lukas, G. Witte, and Ch. Wöll, *Phys. Rev. Lett.* **88**, 028301 (2002).
- ¹⁹C. M. Whelan, M. R. Smyth, C. J. Barnes, N. M. Brown, and C. A. Anderson, *Appl. Surf. Sci.* **134**, 144 (1998).
- ²⁰D. Zerulla, I. Uhlig, R. Szargan, and T. Chasse, *Surf. Sci.* **402**, 604 (1998).
- ²¹L. S. Pinheiro and M. L. A. Temperini, *Surf. Sci.* **441**, 45 (1999).
- ²²Maria Cristina Vargas, Paolo Giannozzi, Annabella Selloni, and Giacinto Scoles, *J. Phys. Chem. B* **105**, 9509 (2001).
- ²³G. Contini, V. Di Castro, A. Angelaccio, A. Sgarlata, and N. Motta, *Surf. Sci.* **470**, L7 (2000).
- ²⁴G. Contini, A. Ciccioli, C. Laffon, Ph. Parent, and G. Polzonetti, *Surf. Sci.* **412/413**, 158 (1998).
- ²⁵V. Carravetta, G. Contini, O. Pashkevych, H. Agren, and G. Polzonetti, *J. Phys. Chem. A* **103**, 4641 (1999).
- ²⁶G. Contini, V. Di Castro, S. Stranges, R. Richter, and M. Alagia, *J. Phys. Chem. A* **104**, 9675 (2000).
- ²⁷Valeria Di Castro, Francesco Allegretti, Chiara Baldacchini, Maria Grazia Betti, Giorgio Contini, Valdis Corradini, Francesca Lamastra, and Carlo Mariani, *Surf. Sci.* **507–510**, 7 (2002).
- ²⁸J. J. Yeh and I. Lindau, *At. Data Nucl. Data Tables* **32**, 1 (1985).
- ²⁹Gay G. Tibbetts, James M. Burkstrand, and J. Charles Tracy, *Phys. Rev. B* **15**, 3652 (1977).
- ³⁰D. T. Ling, J. N. Miller, D. L. Weissman, P. Pianetta, P. M. Stefan, I. Lindau, and W. E. Spicer, *Surf. Sci.* **124**, 175 (1983).
- ³¹S. E. Anderson and G. L. Nyberg, *J. Electron Spectrosc. Relat. Phenom.* **52**, 735 (1990).
- ³²P. A. Agron, T. A. Carlson, W. B. Dress, and G. L. Nyberg, *J. Electron Spectrosc. Relat. Phenom.* **42**, 313 (1987).
- ³³W. Shen, G. L. Nyberg, and J. Liesegang, *Surf. Sci.* **298**, 143 (1993).
- ³⁴J. L. Domange and J. Oudar, *Surf. Sci.* **11**, 124 (1968).
- ³⁵H. C. Zeng, R. A. McFarlane, and K. A. R. Mitchell, *Phys. Rev. B* **39**, 8000 (1989).
- ³⁶E. Vlieg, I. K. Robinson, and R. McGrath, *Phys. Rev. B* **41**, 7896 (1990).
- ³⁷M. L. Colaianni and I. Chrokendorff, *Phys. Rev. B* **50**, 8798 (1994).
- ³⁸Y. Ma, P. Rudolf, E. E. Chaban, C. T. Chen, G. Meigs, and F. Sette, *Phys. Rev. B* **41**, 5424 (1990).
- ³⁹S. D. Kevan and D. A. Shirley, *Phys. Rev. B* **22**, 542 (1980).
- ⁴⁰P. L. Wincott, N. B. Brookes, D. S.-L. Law, and G. Thornton, *Phys. Rev. B* **33**, 4373 (1986).
- ⁴¹H. Bross and M. Kautzmann, *Phys. Rev. B* **51**, 17 135 (1995).
- ⁴²S. C. Wu, C. K. C. Lok, J. Sokolov, J. Quinn, Y. S. Li, D. Tian, and F. Jona, *Phys. Rev. B* **39**, 13 218 (1989).
- ⁴³M. G. Betti (private communication).